Forest stand age classification using time series of photogrammetrically derived digital surface models

Mikko Vastaranta[1,2*], Mikko Niemi[1,2], Michael A. Wulder[3], Joanne, C. White[3], Kimmo Nurminen[4], Paula Litkey[4], Eija Honkavaara[4], Markus Holopainen[1,2] and Juha Hyyppä[2,4]

Affiliations, addresses:
[1] Department of Forest Sciences, University of Helsinki, P.O. Box 27, FI-00014 Helsinki, Finland
[2] Centre of Excellence in Laser Scanning Research, Finnish Geospatial Research Institute FGI, Geodeetinrinne 2, FI-02430 Masala, Finland
[3] Canadian Forest Service (Pacific Forestry Centre), Natural Resources Canada, 506 West Burnside Road, Victoria, BC, V8Z 1M5, Canada
[4] Finnish Geospatial Research Institute FGI, Geodeetinrinne 2, FI-02430 Masala, Finland

Keywords: Time Series, Image Matching, Forestry, Photogrammetry, Lidar, Forest management
*Corresponding author. Email: mikko.vastaranta@helsinki.fi

Pre-print of published version.
Reference
Vastaranta, M., Niemi, M., Wulder, M.A., White, J.C., Nurminen, K., Litkey, P., Honkavaara, E., Holopainen, M., & Hyyppä, J. 2015. Forest stand age classification using time series of photogrammetrically derived digital surface models. Scandinavian Journal of Forest Research, DOI: 10.1080/02827581.2015.1060256

DOI
10.1080/02827581.2015.1060256

Abstract

In this research, we developed and tested a remote sensing based approach for stand age estimation. The approach is based on changes in the forest canopy height measured from a time series of photo-based digital surface models (DSMs) that were normalized to canopy height models (CHMs) using an airborne laser scanning (ALS) derived digital terrain model (DTM). Representing the Karelian countryside, Finland, CHMs from 1944, 1959, 1965, 1977, 1983, 1991, 2003 and 2012, were generated and allow for characterization of forest structure over a 68-year period. To validate our method, we measured stand age from 90 plots (1256 m^2) in 2014, whereby producer's accuracy ranged from 25.0% to 100.0% and user's accuracy from 16.7% to 100.0%. The wide range of accuracy found is largely attributable to the quality and characteristics of archival images and intra-stand variation in stand age. The lowest classification accuracies were obtained for the images representing the earliest dates. For forest managers and agencies that have access to long term photo archives and a detailed DTM, the estimation of stand age can be performed, improving the quality and completeness of forest inventory data bases.

Introduction

Stand age is an important attribute in forestry. Knowledge of stand age is required, for example, to make growth predictions, to inform on the timing of forest management operations, such as thinnings and renewal cuttings, as well as the maintenance of age diversity across a given forest management area. Stand age is also correlated with growing stock volume and biomass (e.g. Lehtonen et al. 2004). Additionally, given stand height and age information, site type can be estimated by using site index curves (Holopainen et al. 2010c; Véga and St-Onge 2008; 2009).

Stand age can also be determined by borings or counting whorls from sample trees, which each being a laborious and time consuming element of field inventories (Bradford et al. 2008; Racine et al. 2014; Véga & St-Onge 2008). When using these methods, a conversion factor is required to convert age at breast height to a biological age. Stand age can be also determined based on time since last disturbance (Bradford et al. 2008) such as stand-replacing fire, wind damage, or clear-cut. If the forest area is managed, disturbance or stand renewal information can theoretically be obtained accurately from forest information registers if the relevant information on stand establishment or stand replacing disturbance has been recorded. Many of these stand age determination methodologies include some element of uncertainty or particular limitations. If the stand age is obtained using an increment borer, it is often done only for a single sample tree within a stand (typical stand sizes varies from 0.5 ha to 15 ha), for which the selected tree age may differ markedly from the stand's mean age. Stand age can only be calculated from the whorls in young pine stands. Stand register information can be of variable quality and completeness (e.g. Holopainen et al. 2010b); with, for example, different methods for the stand age reported in the stand register are implemented, including boring, date of renewal cutting, or through a visual inspection.

Forest resource information is increasingly obtained using remote sensing. In many jurisdictions, standwise field inventories have been replaced by an airborne laser scanning (ALS) based inventory method in which forest inventory attributes are statistically predicted for the area of interest (Hyyppä et al. 2008; Næsset et al. 2004). Field information need only be collected for sample plots that are used to create predictive models. The predictive models from the co-located sample plots and grid-based summaries of the ALS data allow for area-wide mapping of forest attributes. Stand information is summed from the grid cells when required (White et al. 2013a). To extend the attribute set available from ALS and remote sensing, there is interest in the development of new methods for obtaining stand age at the grid cell resolution (Holopainen et al. 2014; Racine, et al.

2014). There is an asymptotic relationship between stand age and remotely sensed spectral variables (Niemann 1995). Younger stands, prior to crown closure, can be characterized with some success; older, more mature stands remain problematic (Duncanson et al. 2010). Time series of satellite data can offer a means for capturing change and reporting time since disturbance (Croft et al. 2014; Kennedy et al. 2009) that could be further used in the estimation of the stand age (Bradford et al. 2008). ALS provides accurate direct measures of tree and stand height (Hyyppä et al. 2012). The link between tree and / or stand age with measured heights has shown promise, but is also quite variable due to variations in forest management, site fertility and other growing conditions, such as climate, water and light availability often confounding this inference (Kalliovirta & Tokola 2005; Racine et al. 2014; Véga & St-Onge 2009). For example, Kalliovirta and Tokola (2005) developed models for predicting tree age using field measured tree height and crown diameter as predictors. The predictors were selected in a way that those could be measured using aerial images or ALS. The root mean squere errors (RMSEs) of the developed models varied between 9.2% and 12.8% (6.1-7.5 years) depending on the used predictors and tree species.

While dependent upon the nature of forest management practices being implemented, when using predictive question that require site index, errors of 5 years have been demonstrated to dramatically influence the predicted site type (Holopainen et al. 2010c) and modeled outcomes. When using site type in forest management planning calculations (e.g., growth prediction and renewal cutting optimization) errors in stands age should be minimized to decrease uncertainty in decision making (Holopainen et al. 2010a; Holopainen et al. 2010d). Thus, the current stand age predictions are often considered to be too uncertain to be of practical value in forest management (Maltamo et al. 2009; Racine et al. 2014).

ALS or aerial stereo-imagery can be used to create digital surface models (DSMs; White et al. 2013b). Besides the characterization of above found vegetation, ALS pulses are capable of penetrating through vegetation to the ground surface enabling accurate characterization of ground height and the production of accurate digital terrain models (DTM). Due to occlusion and shadowing, stereo-imagery is not as well suited and capable of mapping ground height in forested areas (Vastaranta et al. 2013). However, in conjunction with detailed ALS-derived DTM, DSMs created with stereo-imagery can be normalized to represent tree heights (White et al. 2013b). The ALS-derived DTM provides the baseline ground measurement, with the stereo-image derived DSM capturing the upper canopy envelope. Improved automatic stereo-image processing, openly available historic image archives and ALS-based DTMs have enabled production of time-series of canopy height models (CHMs) retrospectively (via differencing of the baseline DTM with the photo-derived DSMs). This kind of time-series is well suited to capturing forest structural development over time and is based on assumption that the ground level has remained largely unchanged over time, which is a reasonable assumption for most regions. Locations with more variability in terrain where landslides, slumping, or other geomorphic or geological considerations may be present would require additional attention/consideration prior to implementation.

Fujita et al. (2003) and Itaya et al. (2004) analyzed canopy gap dynamics and height changes over 32-years in an old-growth evergreen broadleaved forest in Japan. They used measurements from a transit compass and global navigation satellite system (GNSS) to obtain ground elevation and aerial photographs to create DSMs and further CHMs with a spatial resolution of 2.5 m for four different points in time. With a detailed ALS derived DTM, similar time-series of CHMs were generated over 58-years by Véga and St-Onge (2008). Véga and St-Onge (2009) further used CHM-derived time-series for mapping of site index and age by linking multitemporal CHM information with growth curves. In forestry, besides canopy dynamic studies and estimation of site index, there are possibilities for practical applications in many cases only possible based upon time series of canopy height information derived from historical photo archives. Looking forward, many jurisdictions are periodically collecting ALS data and on a more regular basis continue to obtain aerial images providing the source information for time-series generation and novel applications in the future.

In this research, we developed and tested an approach for stand age estimation using a combination of ALS-derived DTM and DSMs created using photos from an image archive. Our approach is based on determining time since last disturbance, which in managed boreal forest conditions found from Finland, this is usually equal to time since stand renewal via clear-cut harvest. Availing upon existing photo archives, we produced multiple photo-based CHMs to map the time of the stand renewal and used that information for stand age classification. Our hypothesis was that stand renewal result in a dramatic contrast in the height metrics calculated from the CHM and that the change reveals the date of renewal. Our time series included CHMs from eight different time periods between 1944 and 2012.

Materials and Methods

Study area and sample plot measurements

The study area covered 37.8 km^2 in the Palokangas, Ilomantsi, found in the eastern corner of Finland (62°53′N, 30°54′E, Figure 1). Dry to dryish forest site types dominate the region. Scots Pine (*Pinus Sylvestris* L.) is the most common tree species in the area.

The ground plots were sampled using existing stand register information that was obtained from Tornator Oyj (Imatra, Finland). The information had been collected using stand wise field inventory, with procedures following Koivuniemi and Korhonen (2006). The sampling was targeted to Scots pine-dominated stands with a maximum stand age of 70 years (i.e., stand established in 1944), growing in productive forest land, (i.e., the volume growth was at least 1 m^3 ha^{-1} per year). The stands were divided to three strata (5–25, 26–50, and 51–70 years) to distribute plots roughly over representative age classes. Then, circular plots with a radius of 20 meters (1256 m^2), were established at the geometric centroid of the selected stands.

In total, 90 plots were measured in the field. The field measurement campaign was carried out in August of 2014. The field plots were located with a hand held GNSS device (Trimble Pro 6T receiver) and the locations were post-processed using virtual reference station data. The forest site type following Cajander (1926) was defined for all the plots, and most of the plots (84 of 90) were located in dry or dryish site types. Stand age at the breast height was measured by boring a tree representing the dominant canopy layer and counting annual rings to determine age. As an exception, in young pine stands age was estimated by counting whorls following standard measurement practices for small trees. Established conversion factors were added to convert age at breast height to biological age. In the study area, the conversion factors used varied from 13 years to 20 years depending on the site type (Heikkilä et al. 2011).

We also collected a sample to evaluate the intrastand variation in the age. For this purpose 24 plots were systematically sampled out of 90 plots and five trees per sample plot were measured; one tree from the center of the plot and the other trees from 20 meters to every cardinal direction from the sample plot center. In 12 out of these 24 plots, stand age was measured by boring and in 12 plots, stand age was measured from whorls, based upon the maturity of the trees present.

Figure 1. Study area and location of the sample plots on an aerial image (Copyright for aerial images: National Land Survey of Finland©).

Airborne images

The airborne images covered a time interval from 1944 to 2012. A digital camera was used in the 2012 collection, with film cameras used for the rest of the image time series. The images were mostly panchromatic and collected in June and July (leaf-on) at altitudes varying from 4 km to 8 km. All of the images were originally collected for national level topographic mapping by the National Land Survey of Finland (NLS) (data sets of 1977, 1983, 1991, 2003, and 2012) and the Finnish Defense Intelligence Agency (data sets of 1944, 1959, and 1965). The NLS is currently scanning the entire historical image archive in Finland. From year 2000 Leica DSW photogrammetric scanners have been used. Scanning pixel size was 15 µm or 20 µm, providing ground sample distances (GSDs) of 0.45-0.88 m. Further details of the image blocks are given in Table 1 and 2.

Table 1. Details of the image blocks used. FH: Flying height above the average ground level; FD: major flight direction: NS=North-South, EW=East-West; Overlaps: p=forward overlap; q=side overlap

Table 2. Camera information. FOV: image field of view at format corner.

Digital terrain model

An ALS-derived digital terrain model (DTM) with a one meter horizontal grid resolution was available for the study area. The DTM was based on ALS data that was acquired for research purposes in October 2008 with a Leica ALS50-II SN058 laser scanner (Leica Geosystem AG, Heerbrugg, Switzerland). The data acquisition parameters include: flying altitude of 500 m at a speed of 80 knots, 30 degrees field of view, pulse rate of 150 kHz, scan rate of 52 Hz, laser footprint size of 0.11 m, and pulse density of 20 pulses per m^2. The DTM was processed from the point cloud using standard approaches, with ALS data first classified into ground or non-ground points allowing for DTM creation using the classified ground points (Axelsson 2000).

General methodological workflow

To summarize, the aim is to classify forest stand age by using a time series of image-based DSMs (from archival air photos) and a single time-point DTM (from ALS). DSMs were processed from aerial images and normalized to CHMs using the DTM. To derive DSMs from image archives an automatic processing chain was developed by Nurminen et al. (2015). In this process, initially the interior and exterior orientation of the images is determined. Then images are matched to produce DSMs. Then, specific to our approach, forest stand age was then determined by searching the time series for the change point where the height of the stand changed notably revealing the occurrence of a stand replacing disturbance. Finally, we evaluated stand age classification accuracy using field measured stand age data as a reference. In addition, the field measured stand age data was visually verified from the images further increasing the accuracy of the reference.

Processing of the aerial imagery

We used the BAE Systems SOCET SET V5.6.0 software (Walker 2007) to implement the required photogrammetric production environment. For initial values of exterior orientation in the most difficult cases, VisualSFM software (Wu 2013; Wu et al. 2011) was used. In addition some in-house software was used (for details, see Nurminen et al. 2015).

Interior orientation

The interior orientation is the transformation between the image measurement coordinate system and the camera coordinate system. The required information for performing this transformation is generally provided in a camera calibration certificate. In our case, the required information was available for the images acquired since 1965. For the recent images obtained by digital camera this transformation is considered constant for each image related to the same camera calibration. For the interior orientation, we used the affine model as the geometric transformation model. The residuals of the affine model were less than 10 microns for all the image blocks except for the image block captured in 1944 (~40 microns).

Exterior orientation

Exterior orientation means the location of the image projection center and the rotations of the image plane with regards to the chosen ground coordinate system. VisualSFM software (Wu 2013; Wu, et al. 2011) was used for the initial exterior orientation of image blocks that did not have accurate *a priori* exterior orientations and camera calibrations (1944 and 1959 images). With only five interactively measured GCPs these image blocks were transformed to Finnish ETRS-TM35FIN N2000 coordinate system. Later, additional GCPs were interactively measured for these two earliest image blocks in SOCET SET software. For 1965, 1977, 1983, 1991, and 2012 datasets an interactive procedure was used to determine a priori orientations. The approximate horizontal image locations were measured from open topographical data or using a calculated planar rectification. For the 2003 image set approximate exterior orientations were available. Then automatic tie points and the required GCPs were measured before bundle block adjustments. Finally, self-calibrating bundle block adjustments were calculated. Based on quality statistics of bundle block adjustment, RMS-errors of the GCPs varied between 1.4 m-1.9 m in XY and 1.0 m-2.1 m in Z in image blocks 1944, 1959 and 1965. After 1977 the RMS-errors of the GCP were found to have dropped and were in general between 0.5 m and 1.0 m.

DSM generation

DSMs with 1 m resolution were generated by image matching using an area based matching method and a matching strategy suitable for finding spatial agreement in an environment with large height differences, such as forest. At maximum, three image pairs per point were used. Accuracy of the DSMs was evaluated using ALS DTM where roads are present. The standard deviation of heights varied from 0.4 m (2012) to 1.6 m (1944) in road surfaces (width >3m) indicating a proportional height error of approximately 0.2–0.25‰ of the flying height for the older blocks and 0.1‰ or better of the flying height for the new blocks (since 1977). These results are consistent with the expected level of accuracy for photogrammetric elevation measurements (Kraus 1993). CHMs were generated by subtracting the DTM from DSMs.

Stand age determination using time series data

We developed a method that uses the year of discernable previous clear-cut to determine the stand age. The most common stand renewal method has been a clear-cut in Finland since the 1950's (Jalonen & Vanha-Majamaa 2001). After the harvest, following national regulations for sustainable forest management, the forest is to be regenerating naturally or via artificially (cultivation, planting) intervention within the next three to five years according to Finnish Forest Act (1996). Detailed CHMs provide information from the canopy structure and related development and change (Vastaranta et al. 2013). Under non-disturbed stand growth conditions, the CHM-derived stand mean and maximum height would generally show small positive changes. In boreal forest conditions, especially in our pine-dominated study area, CHM minimum values originate from the ground surface. The standard deviation of the heights would also increase as the height of the trees increases, with observations originating from the ground and from the tops of trees. Clear-cut of the stand would, as such, result in an abrupt decrease in both mean and maximum heights; additionally, a decrease in the standard deviation of the heights should also be detectable.

Hence, to determine stand age, we used a stepwise procedure with the CHM time series data. Descriptive height statistics were calculated for sample plots (1256 m^2) using the CHMs. Statistics included minimum, maximum, mean, and standard deviation of the CHM (Table 3) for all the stands and for all the time-points. Overall, our data included eight stand age classes (Table 4) that were defined by acquisitions of the various epochs of images available. In our approach, we iterated through the CHM-derived metrics (mean, max, std) and determined the time-interval of the clear-cut as follows:

1) Height metric_{Tn}-Height $\text{metric}_{Tn+1} > \text{Threshold}_1$, and

2) Height $\text{metric}_{Tn+1} < \text{Threshold}_2$.

For example, if CHM-derived maximum height in 1983 is 20 m and 1m in 1991, it means there is decrease of 19 m in height between the years indicating a notable change. An additional criterion (2) was added to ensure that the canopy height decreased below a given threshold height. Then independent optimal threshold values that maximized stand age classification accuracy were selected for mean, max, and std of CHM values. The accuracy of the stand age determination was evaluated using the aforementioned field measurements and reported in a contingency table.

Table 3. Descriptive statistics of the height metrics extracted from CHM time series for 90 sample plots (1256 m^2).

Table 4. Stand age classes

Results

Stand age determination in the field

Based on our field measurements, the stand ages varied from 5 to 94 years (mean = 38 years, standard deviation = 24.7 years). The number of stands within each stand age class varied with only two stands found to be regenerated between 1944 and 1959 compared with 28 stands that were regenerated between 1991 and 2003. The accuracy of our stand age field measurements was assessed by measuring stand age from 5 sample trees per plot and analyzing the variation and range in stand age measurements. Standard deviation of the stand age measurements within sample plots was 5.1 years and the average range was 12.3 years. In sample plots where stand age was measured by counting whorls, stand age was on average 40.0 years. Standard deviation of the stand age measurements within sample plots was only 2.0 years as the average range was 4.7 years indicating these stands have a more homogeneous age structure which is presumable within this rather limited stratum (i.e. this technique is only possible in relatively young pine stands). We compared the stand age information from the existing stand register to our stand age measurements. On average, stand age obtained from the register was three years younger with standard deviation of 12 years. However, the range of errors was ±25 years in general, indicating large variation in stand age accuracy (Figure 2). In addition, we visually verified the time of the renewal. During that process, we altered age class of 25 stands.

Figure 2. Differences between the field-measured stand age and stand age obtained from existing stand register.

Stand age classification using time series data

CHM time series data was used to determine time of the previous clear-cut and consequently stands age class. In figure 3, stand height development in example stands is presented using the time series information. The best overall classification accuracy was 78.9% and it was obtained using changes in maximum heights (Figure 4, Table 5). Optimal parameter values for threshold_1 and threshold_2 were 5-6 m and 11 m, respectively. In other words, the best classification accuracy was obtained when stand maximum height was decreased by at least 5 meters between T_n and T_{n+1} and maximum height was below 11 meters at T_{n+1}. In general, it should be noted that the accuracies obtained with changes in standard deviations or mean heights were only slightly lower. There was a wide range in accuracy between the stand age classes. Producer's and user's accuracies varied from 25.0% to 83.3% and 16.7% to 83.3% in stands that were regenerated before 1991. Stands that were renewed after 1991 were all classified correctly. With our approach, mapped stand age classes generally followed current stand boundaries. This partly indicates within stand age variation caused by, for example, seed tree or shelterwood cuttings (Fig. 5).

Figure 3. Two examples of the CHM time series data. On the left side the plot has been harvested 1994 according the field measurements and the level of CHM have clearly lowered between 1991 and 2003. On the right side the plot represents a typical error in the analysis before visual verification, as the clear-cut was determined to have occurred in 1958 by field measurement, but the CHM data clearly points out that a clear-cut was done between 1959 and 1965.

Figure 4. Age classification using height statistics derived from CHM.

Table 5. The age classification matrix using the image time-series. The stand regeneration time was defined using change statistics derived from CHM. Here, stand regeneration was defined using following parameters: Stand maximum height was decreased at least 5 meters between T_n and T_{n+1} and maximum height was below 11 meters at T_{n+1}.

Figure 5. Example of the mapped stand age classes using time series of photogrammetrically derived DSMs. Aerial image from 2012 on the background (Copyright for aerial images: National Land Survey of Finland©).

Discussion

Remote sensing is commonly used to collect information over vast forest areas. Stand age is an important forest characteristic for many management applications although it is known to be challenging to estimate without field visits (e.g., Maltamo et al. 2009; Holmström et al. 2010; Racine et al. 2014). Following the developed time-series method herein, we obtained an overall classification accuracy of 78.9% using changes in maximum heights. Considerable variation in accuracy was detected between the stand age classes. Stands that were renewed after 1991 were all correctly classified. When estimating age of the older stands, far lower classification accuracies were obtained. Presumably lower classification accuracies are caused by two main reasons. Firstly, the quality of the old archived images is lower than in ones that are currently in use; this impact diversely to the quality of DSMs and automatic interpretation. The lower image quality is seen as poorer contrasts, higher noise levels and greater geometric distortions and it is due to poorer quality of cameras, film used, and overall systems utilized in historic data as well as due to the distortions in films due to ageing (Nelson et al. 2001; Nurminen et al. 2015). Secondly, our ground reference age obtained by boring a single tree, includes more uncertainty, because annual growth rings are more challenging to measure. However, the effect of this error source was reduced by visual interpretation of the images. The time between the image acquisitions varied from 6 to 15 years. From the two thresholds used, $threshold_1$ is affected by the time span. We also tested height changes per year (detected change normalized by number of years), but it did not improve the classification accuracies. We assume that has to be due to rather robust parameters: $Threshold_1$ determines simply that there has to be a decrease in the canopy height. Then $threshold_2$ determines that the height of the canopy must be below certain height limit.

Looking forward, many jurisdictions report intentions and programs to continue to collect digital photography on a regular and increasingly routine basis (Holopainen et al. 2014). In these cases time-series-based stand age determination could be applied. With narrow time-windows between the image acquisitions, stand age can be presumably estimated with accuracy improving the forest inventory, management, and planning. Considering that the image acquisition time-interval was ~10 years and first images were acquired in 1944 in our data, the obtained accuracy (78.9%) is still comparable with other remote sensing based age estimates that have been obtained with aerial images (Holmström et al. 2010) or single time point ALS (Maltamo et al. 2009; Racine, et al. 2014). Holmström et al. (2010) used interpretation of aerial photographs and nearest neighbor estimation to predict stand age and obtained 15% RMSE at the stand level. Maltamo et al. (2009) predicted stand age using national forest inventory sample plots and ALS data using k-MSN imputation approach. The RMSEs for Scots pine and Norway spruce at the plot and stand level was found to vary from 16.7 years to 23.5 years, respectively. Racine et al. (2014) predicted stand age using ALS-derived forest structural variables (e.g., height metrics, penetration of the laser pulses) and site attributes (e.g., elevation, slope, and aspect) as predictors in nearest neighbor imputation. The stand prediction error obtained was less than 10 years (RMSE 19%) indicating that forest height is well correlated with stand age although there remains some level of uncertainty.

Nurminen et al. (2015) demonstrated that with historical (i.e., before 1960) imagery, it is difficult to achieve a DSM accuracy level common to modern large-format aerial cameras. However, following a thorough self-calibration during the bundle block adjustment and by carefully reconstructing the missing camera calibration, it was possible to obtain forest canopy height information of a feasible quality; the height errors in well-defined targets were 0.3–0.9 m for the datasets collected since 1970 and for the older datasets, they were 1–2 m. These values indicated a proportional height error of approximately 0.2–0.25‰ of the flight height for the older blocks and 0.1‰ of the flight height or better for the new blocks. Detailed DTMs have been available only since ALS has become common in the 2000's (Hyyppä et al. 2008; Hyyppä et al. 2009; Wulder et al. 2013). Thus, when obtaining retrospective canopy heights from DSM time series, one must assume that ground level has remained largely unchanged over time.

Defining stand origin can be challenging and cause uncertainty to stand age estimation. There are many definitions in use and it depends on the information need. In Finland, forests have to be regenerated after the cutting using natural or artificial (cultivation, planting) methods within three to five years following harvest according to the Finnish Forest Act (1996). Thus, if the time of the previous cutting can be mapped, it can be used to determine stand age rather accurately, as we have demonstrated, especially so in younger stands. This finding cannot be generalized to the other areas with different forest management practices. However, on the other hand, time-series of CHMs can be also used to map time when a canopy height reaches some predefined threshold and that can be used as stand origin after adding some conversion factor respective to the age at the breast height conversion factors.

Following common practices, stand age was measured using an increment borer with reference measures obtained by boring a single dominant tree. The correct age class was further ensured by visual interpretation of the imagery, because in some stands, the reference stand age did not agree with the drastic decrease in CHM (e.g., Figure 3 right panel). It is also noted that we measured within stand variation of 5 years (Std) and range of 12 years in age. In addition, a conversion factor was added to convert age at the breast height to biological age. This may also cause some uncertainty. In our approach, stand age was defined as a time since last disturbance. Bradford et al. (2008) aimed to determine the relation between the time since disturbance and measured tree age (boring). They concluded that in mainly natural, sub-alpine forest located in the Southern Rocky Mountains, observed tree age was poor predictor for time since disturbance. However, the forest management and the stand renewal patterns in Finland are far more controlled. In our case, it was safe to assume that the disturbance was always a clear-cut and new stand was established only few years after the cutting which is determined by common practice and enforced by Finnish forest legislation. During the visual verification from the imagery, we detected only two other regeneration systems than clear-cuts (shelterwood cuttings). Both of these stands were misclassified by our approach.

The method was validated using sample plots (1256 m^2) from which the stand age were obtained as well. In other words, the validation resolution was already at "sub-stand level", but coarser that what is currently used when forest inventory attributes are predicted using ALS data and field plots. When ALS-based forest inventory is applied in Finland, the prediction resolution is 256m^2. However, our method is not depended on stand boundaries and can provide thematic maps of stand age to be used with other forest attribute maps in forest management.

We used small scale airborne image archives in our investigation, which are available since World War II in many developed countries. The interesting aspect with the small scale data is that it is possible to provide DSM time series covering entire countries and over large areas, providing the presence of ALS data for DTM generation. Larger-scale materials are also available (Korpela 2006; Véga & St-Onge 2008; 2009); these images provide improved height accuracy, but their areal extent is not in most cases as large as of the small-scale archives. Satellite imagery, such as from Landsat, can provide dense time series change information over large areas and may prove compatible with our approach to offer additional disturbance information to support the mapping of time since disturbance.

For forest managers and agencies that have access to long-term photo archives and a detailed DTM, the estimation of stand age can be performed using time-series characterizations of canopy height, improving the quality and completeness of forest inventory data bases. The utility of the time-series-based forest stand age determination is dependent on time interval and quality of the images available. In addition, accuracy is affected by forest management practices such as practices and regulations associated with ensuring post-harvest regeneration. Based on our analyses, aerial images acquired after 1991, provided accurate stand age classifications.

Acknowledgements

The authors are grateful to National Land Survey for scanning the images for this investigation and for the open topographic datasets: national digital terrain model, orthophoto and Topographic Database. The authors also acknowledge the Finnish Defence Intelligence Agency for the film materials dating 1944, 1959 and 1965. The research carried out in this study was financially supported by the Academy of Finland (Project No. 273806 and Centre of Excellence in Laser Scanning Research (CoE-LaSR)) and the Finnish Ministry of Agriculture and Forestry (DNro. 350/311/2012). Elements of this research were also supported by the Canadian Wood Fibre Centre (CWFC) of the Canadian Forest Service, Natural Resources Canada.

References

Act F. 1996. Metsälaki [Forest Act]. N: o.1093:12.12. Finnish.

Axelsson P. 2000. DEM generation from laser scanner data using adaptive TIN models. Int Arch. Photogramm. Remote Sens. 35: 236-241.

Bradford JB, Birdsey RA, Joyce LA, Ryan MG. 2008. Tree age, disturbance history, and carbon stocks and fluxes in subalpine Rocky Mountain forests. Glob Chang Biol.14:2882-2897.

Cajander A. 1926. The theory of forest types. Acta For Fenn. 29: 1-108.

Croft H, Chen J, Noland T. 2014. Stand age effects on Boreal forest physiology using a long time-series of satellite data. For Ecol Manage. 328:202-208.

Duncanson LI, Niemann KO, Wulder MA. 2010. Integration of GLAS and Landsat TM data for aboveground biomass estimation. Can J Remote Sens. 36:129-141.

Fujita T, Itaya A, Miura M, Manabe T, Yamamoto SI. 2003. Long-term canopy dynamics analysed by aerial photographs in a temperate old-growth evergreen broad-leaved forest. J Ecol. 91:686-693.

Heikkilä J, Ärölä E, Kilpiäinen S. 2011. Kaukokartoitusperusteisen metsien inventoinnin koealojen maastotyöohje [Field work guide for remote sensing based forest inventory]. Helsinki (Finland): Forestry Development Centre TAPIO, Finnish Forest Centre. Finnish.

Holopainen M, Mäkinen A, Rasinmäki J, Hyyppä J, Hyyppä H, Kaartinen H, Viitala R, Vastaranta M, Kangas A. 2010a. Effect of tree-level airborne laser-scanning measurement accuracy on the timing and expected value of harvest decisions. Eur J For Res. 129:899-907.

Holopainen M, Mäkinen A, Rasinmäki J, Hyytiäinen K, Bayazidi S, Pietilä I. 2010b. Comparison of various sources of uncertainty in stand-level net present value estimates. For Policy Econ. 12:377-386.

Holopainen M, Vastaranta M, Haapanen R, Yu X, Hyyppä J, Kaartinen H, Viitala R, Hyyppä H. 2010c. Site-type estimation using airborne laser scanning and stand register data. Photogramm J Finland. 22:16-32.

Holopainen M, Vastaranta M, Rasinmäki J, Kalliovirta J, Mäkinen A, Haapanen R, Melkas T, Yu X, Hyyppä J. 2010d. Uncertainty in timber assortment estimates predicted from forest inventory data. Eur J For Res. 129:1131-1142.

Holopainen M, Vastaranta M, Hyyppä J. 2014. Outlook for the Next Generation’s Precision Forestry in Finland. Forests 5:1682-1694.

Holmström H, Nilsson M, Ståhl, G. 2010. Simultaneous estimations of forest parameters using aerial photograph interpreted data and the k nearest neighbour method. Scand J For Res. 16:67-78.

Hyyppä J, Hyyppä H, Leckie D, Gougeon F, Yu X, Maltamo M. 2008. Review of methods of small-footprint airborne laser scanning for extracting forest inventory data in boreal forests. Int J Remote Sens. 29:1339-1366.

Hyyppä J, Hyyppä H, Yu X, Kaartinen H, Kukko A, Holopainen M. 2009. Forest inventory using small-footprint airborne LiDAR. In: Shan J, Toth CK. Topographic Laser Ranging and Scanning: Principles and Processing. Boca Raton: CRC Press; p. 335-370.

Hyyppä J, Yu X, Hyyppä H, Vastaranta M, Holopainen M, Kukko A, Kaartinen H, Jaakkola A, Vaaja M, Koskinen J. 2012. Advances in forest inventory using airborne laser scanning. Remote Sens. 4:1190-1207.

Itaya A, Miura M, Yamamoto S-I. 2004. Canopy height changes of an old-growth evergreen broad-leaved forest analyzed with digital elevation models. For Ecol Manage 194:403-411.

Jalonen J, Vanha-Majamaa I. 2001. Immediate effects of four different felling methods on mature boreal spruce forest understorey vegetation in southern Finland. For Ecol Manage 146:25-34.

Kennedy RE, Townsend PA, Gross JE, Cohen WB, Bolstad P, Wang Y, Adams P. 2009. Remote sensing change detection tools for natural resource managers: Understanding concepts and tradeoffs in the design of landscape monitoring projects. Remote Sens Environ. 113:1382-1396.

Koivuniemi J, Korhonen KT. 2006. Inventory by compartments. In: Kangas A, Maltamo M. Forest inventory –methodology and applications. Dordrecht: Springer; p. 271-278.

Korpela I. 2006. Geometrically accurate time series of archived aerial images and airborne lidar data in a forest environment. Silva Fenn. 40:109-126.

Kraus K. 1993. Photogrammetry, Volume 1, Fundamentals and Standard Processes, with contributions by Peter Waldhäusl. Bonn: Dümmlerbuch

Lehtonen A, Mäkipää R, Heikkinen J, Sievänen R, Liski J. 2004. Biomass expansion factors (BEFs) for Scots pine, Norway spruce and birch according to stand age for boreal forests. For Ecol Manage. 188: 211-224.

Maltamo M, Packalèn P, Suvanto A, Korhonen KT, Mehtätalo L, Hyvönen P. 2009. Combining ALS and NFI training data for forest management planning: a case study in Kuortane, Western Finland. Eur J For Res. 128:305-317.

Nelson T, Wulder MA, Niemann KO. 2001. Spatial resolution implications of digitising aerial photography for environmental applications. Imaging Sci J. 49:223-232.

Niemann KO. 1995. Remote sensing of fores stand age using airborne spectrometer data. Photogramm Eng Remote Sens. 61:1119-1127.

Nurminen K, Litkey P, Honkavaara E, Vastaranta M, Holopainen M, Lyytikäinen-Saarenmaa P, Kantola T, Lyytikäinen M. 2015. Automation aspects for the georeferencing of photogrammetric aerial image archives in forested scenes. Remote Sens. 7:1565-1593.

Næsset E, Gobakken T, Holmgren J, Hyyppä H, Hyyppä J, Maltamo M, Nilsson M, Olsson H, Persson Å, Söderman U. 2004. Laser scanning of forest resources: the Nordic experience. Scand J For Res. 19:482-499.

Racine EB, Coops NC, St-Onge B, Begin J. 2014. Estimating Forest Stand Age from LiDAR-Derived Predictors and Nearest Neighbor Imputation. Forest Sci. 60:128-136.

Walker S. 2007. New features in SOCET SET®. In: Fritch D. Proceedings of the Photogrammetric Week; 2007 Sep 3-7; Stuttgart (Germany): University of Stuttgart

Van Laar A, Akça A. 1997. Forest mensuration. Gottingen: Cuvillier Verlag.

Vastaranta M, Wulder MA, White JC, Pekkarinen A, Tuominen S, Ginzler C, Kankare V, Holopainen M, Hyyppä J, Hyyppä H. 2013. Airborne laser scanning and digital stereo imagery measures of forest structure: comparative results and implications to forest mapping and inventory update. Can J Remote Sens. 39:382-395.

Véga C, St-Onge B. 2008. Height growth reconstruction of a boreal forest canopy over a period of 58 years using a combination of photogrammetric and lidar models. Remote Sens Environ. 112:1784-1794.

Véga C, St-Onge B. 2009. Mapping site index and age by linking a time series of canopy height models with growth curves. For Ecol Manage. 257: 951-959.

White JC, Wulder MA, Varhola A, Vastaranta M, Coops NC, Cook BD, Pitt D, Woods M. 2013a. A best practices guide for generating forest inventory attributes from airborne laser scanning data using an area-based approach. Victoria, BC (Canada): Natural Resources Canada, Canadian Forest Service, Canadian Wood Fibre Centre, Pacific Forestry Centre.

White JC, Wulder MA, Vastaranta M, Coops NC, Pitt D, Woods M. 2013b. The utility of image-based point clouds for forest inventory: a comparison with airborne laser scanning. Forests 4: 518-536.

Wu C. Towards linear-time incremental structure from motion. In: Curless B. Proceedings of International Conference on 3D Vision; 2013 Jun 29 – July 1; Seattle. Washington(USA): University of Washington.

Wu C, Agarwal S, Curless B, Seitz SM. Multicore bundle adjustment. In: Proceedings of IEEE Conference on Computer Vision and Pattern Recognition; 2011 Jun 20-25; Colorado Springs, Colorado(USA): Crowne Plaza.

Wulder MA, Coops NC, Hudak A, Morsdorf F, Nelson R, Newnham G, Vastaranta M. 2013. Status and prospects for LiDAR remote sensing of forested ecosystems. Can J Remote Sens. 39:1-5.

Figures

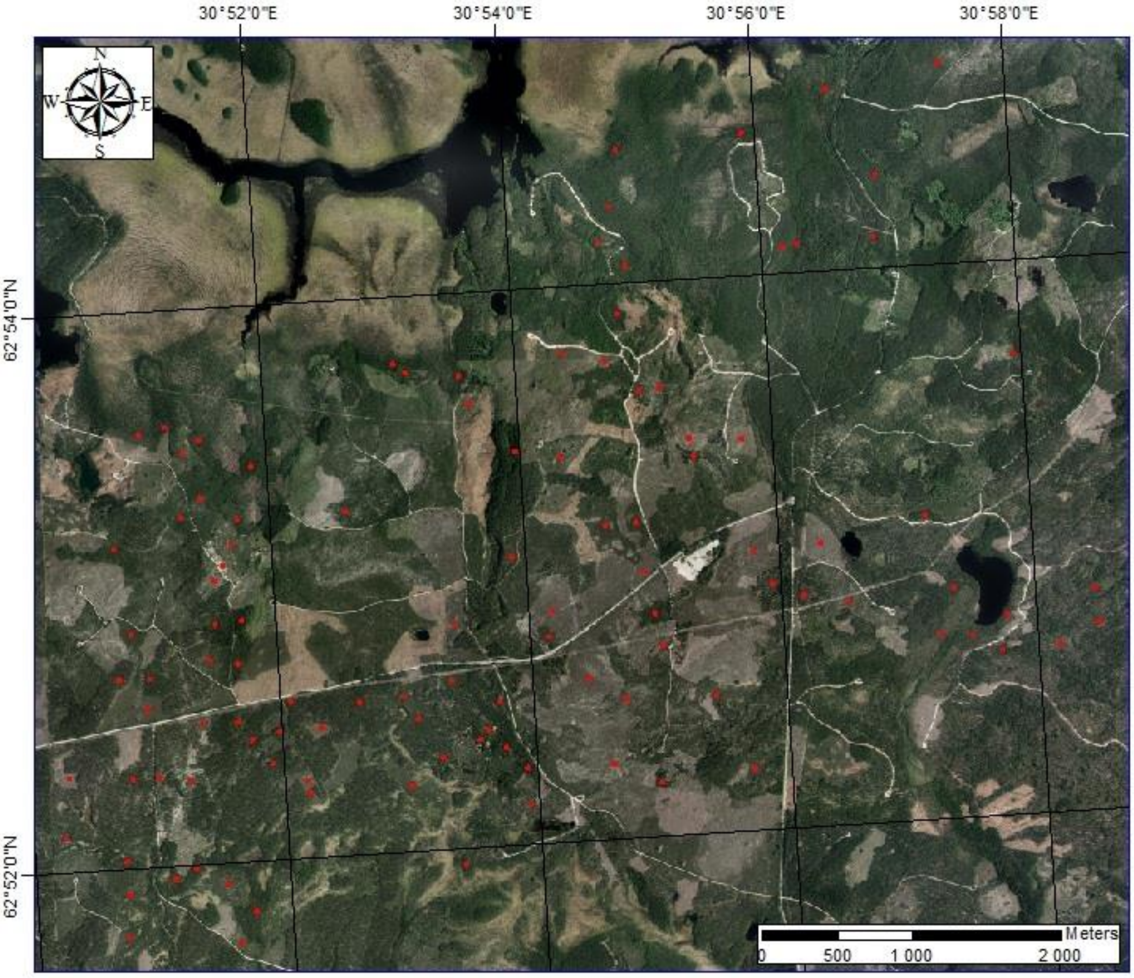

Figure 1. Study area and location of the sample plots on an aerial image (Copyright for aerial images: National Land Survey of Finland©).

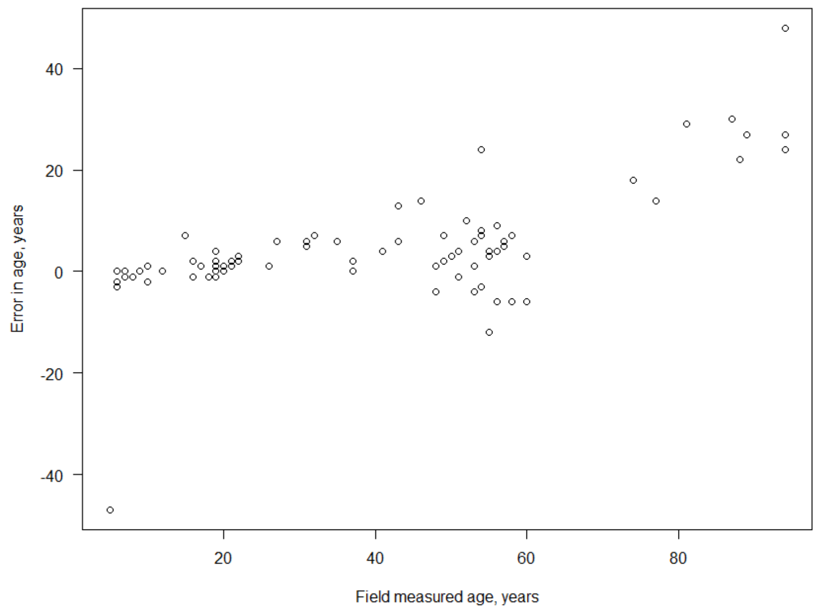

Figure 2. Differences between the field-measured stand age and stand age obtained from existing stand register.

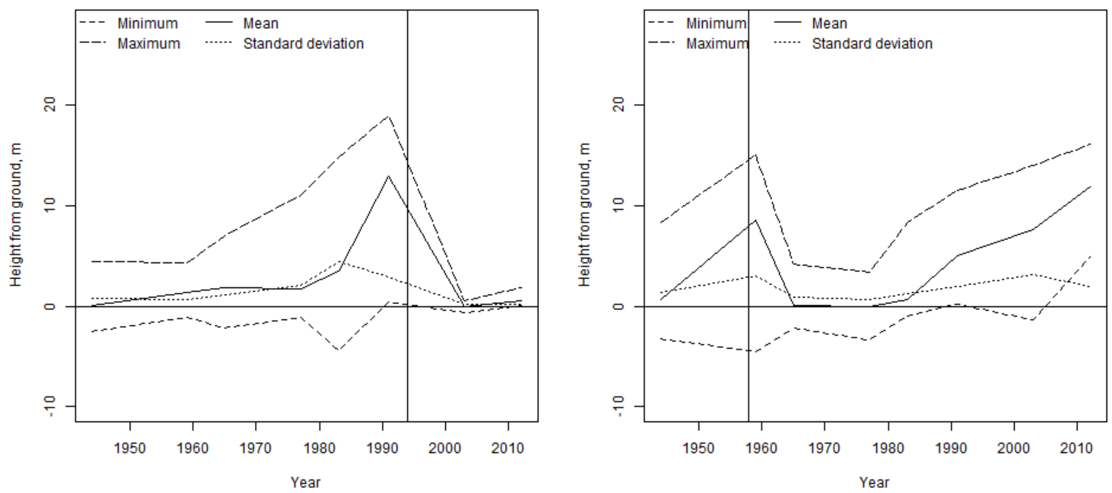

Figure 3. Two examples of the CHM time series data. On the left side the plot has been harvested 1994 according the field measurements and the level of CHM have clearly lowered between 1991 and 2003. On the right side the plot represents a typical error in the analysis before visual verification, as the clear-cut was determined to have occurred in 1958 by field measurement, but the CHM data clearly points out that a clear-cut was done between 1959 and 1965.

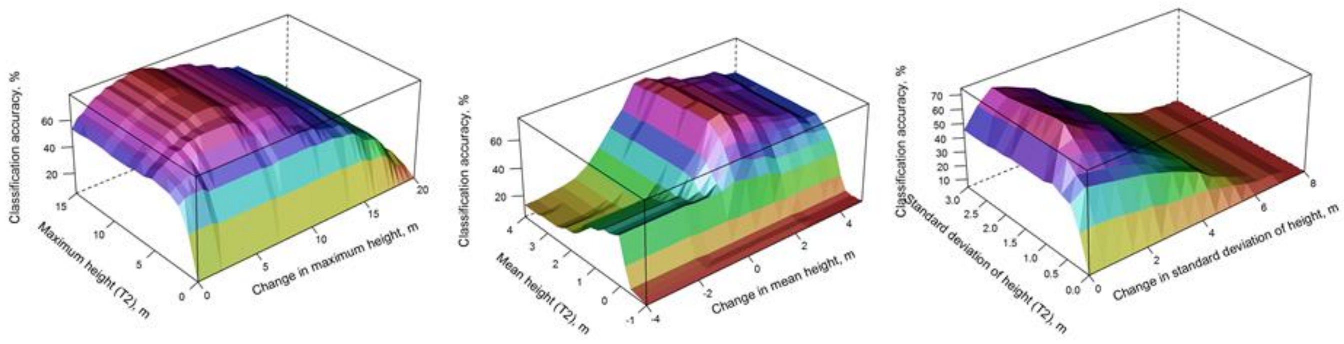

Figure 4. Age classification using height statistics derived from CHM.

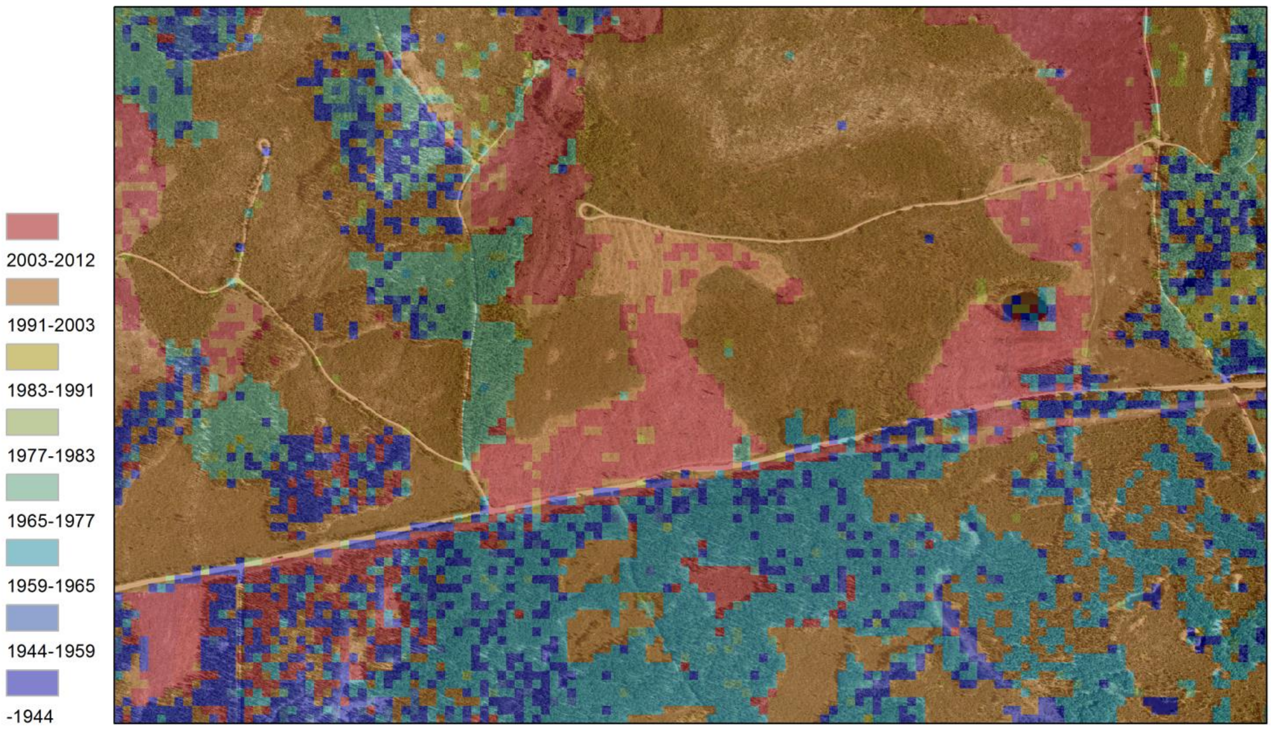

Figure 5. Example of the mapped stand age classes using time series of photogrammetrically derived DSMs. Aerial image from 2012 on the background (Copyright for aerial images: National Land Survey of Finland©).

Tables:

Table 1. Details of the image blocks used. FH: Flying height above the average ground level; FD: major flight direction: NS=North-South, EW=East-West; Overlaps: p=forward overlap; q=side overlap

Date of flight	Scale	FD	Overlaps p;q (%)	GSD (m)	Camera
13.7.1944	1:30K	EW	67, 38	0.45	Zeiss-Aerotopograph RMK HS 1824
22.7.1959	1:40K	NS	67, 36	0.62	Zeiss-Aerotopograph RMK HS 1818
27.7.1959	1:40K	NS		0.61	Zeiss-Aerotopograph RMK HS 1818
4.6.1965	1:60K	NS	79; -	0.88	Carl Zeiss Oberkochen RMK 15/23
11.6.1977	1:31K	EW	59; 39	0.47	Wild Heerbrugg RC10
5.6.1983	1:31K	EW	63; 25	0.45	Wild Heerbrugg RC10A
29.7.1991	1:31K	EW	70; 22	0.63	Wild Heerbrugg RC20
7.6.2003	1:31K	NS	65; 29	0.62	Wild Heerbrugg RC20
16.7.2003	1:31K	NS		0.62	Wild Heerbrugg RC20
14.6.2012	1:75K	NS	60; 30	0.45	Vexcel Imaging UltraCam Xp

Table 2. Camera information. FOV: image field of view at format corner.

Camera name	Lens; f (mm)	Image format (cm)	FOV; +/-°	FMC	Lab. Calibration
Zeiss-Aerotopograph RMK HS 1824	ORTHOMETAR; 204.53	18×18	32	No	NA
Zeiss-Aerotopograph RMK HS 1818	TOPOGON; 100.00	18×18	52	No	NA
Carl Zeiss Oberkochen RMK 15/23	PLEOGON; 152.45	23×23	37	No	1st January 1963
Wild Heerbrugg RC10	NAG II 213.57	23×23	28	No	23rd February 1976
Wild Heerbrugg RC10A	NAG IIA 214.08	23×23	28	No	10th February 1983
Wild Heerbrugg RC20	NAGA-F 214.10	23×23	28	Yes	5th May 1990
Wild Heerbrugg RC20	UAGA-F 153.03	23×23	37	Yes	21st January 2002
Vexcel Imaging UltraCam Xp	100.50	6.786×10.386	32	Yes	18th October 2011

Table 3. Descriptive statistics of the height metrics extracted from CHM time series for 90 sample plots (1256m^2).

Year	Height metric	Mean	Sd	Median	Min	Max
1944	Min	-3.5	1.3	-3.4	-9.6	-1.4
	Max	9.9	4.1	9.7	2.5	19.9
	Mean	0.9	1.9	0.4	-1.8	9.1
	Sd	2.1	1.2	1.7	0.7	6.0
1959	Min	-2.7	3.3	-2.4	-21.1	5.0
	Max	13.0	4.7	14.0	1.4	22.5
	Mean	4.3	3.5	3.5	-0.7	15.3
	Sd	2.9	1.4	2.7	0.5	7.4
1965	Min	-2.9	1.9	-2.8	-6.5	3.1
	Max	10.5	5.4	10.9	1.3	21.7
	Mean	3.2	3.4	2.6	-0.9	13.1
	Sd	2.4	1.4	2.1	0.5	6.5
1977	Min	-2.6	2.4	-2.1	-12.0	3.1
	Max	8.7	6.1	8.3	0.6	21.7
	Mean	2.5	3.4	1.0	-1.0	13.1
	Sd	1.9	1.4	1.5	0.2	5.3
1983	Min	-2.3	2.9	-1.9	-20.3	9.0
	Max	9.0	7.1	6.5	0.6	24.0
	Mean	2.4	4.3	0.7	-0.4	18.1
	Sd	1.8	1.7	1.0	0.2	5.9
1991	Min	-0.3	3.0	-0.2	-6.3	16.5
	Max	12.2	7.0	10.9	0.6	25.5
	Mean	6.4	5.0	5.1	-0.6	20.2
	Sd	2.5	1.9	1.8	0.2	7.7
2003	Min	-0.6	2.5	-0.9	-4.6	12.1
	Max	8.0	6.5	8.6	0.1	21.6
	Mean	3.2	4.1	1.1	-0.5	15.2
	Sd	1.8	1.7	1.2	0.1	7.6
2012	Min	0.0	1.9	-0.1	-7.6	8.2
	Max	8.7	5.9	8.8	0.7	20.1
	Mean	4.1	4.1	2.1	0.2	13.1
	Sd	1.6	1.4	1.3	0.1	5.1

Table 4. Stand age classes

Stand age class	Regenerated	Stand age range in our data based on boring	Number of stands
0	Before 1944	74-94	4
1	Between 1944 and 1959	56-60	2
2	Between 1959 and 1965	50-55	27
3	Between 1965 and 1977	42-49	7
4	Between 1977 and 1983	32-37	5
5	Between 1983 and 1991	26-31	6
6	Between 1991 and 2003	12-22	28
7	Between 2003 and 2012	5-10	11

Table 5. The age classification matrix using the image time-series. The stand regeneration time was defined using change statistics derived from CHM. Here, stand regeneration was defined using following parameters: Stand maximum height was decreased at least 5 meters between T_n and T_{n+1} and maximum height was below 11 meters at T_{n+1}.

Ground reference	Predicted -1944	1944-1959	1959-1965	1965-1977	1977-1983	1983-1991	1991-2003	2003-2012	Row Total Producer's accuracy, %
-1944	1	0	0	0	3	0	0	0	4 25
1944-1959	1	1	0	0	0	0	0	0	2 50
1959-1965	4	2	17	2	1	0	0	1	27 62.9
1965-1977	0	0	0	7	0	0	0	0	7 100
1977-1983	0	0	0	3	1	1	0	0	5 60
1983-1991	0	0	0	1	0	5	0	0	6 83.3
1991-2003	0	0	0	0	0	0	28	0	28 100
2003-2012	0	0	0	0	0	0	0	11	11 100
Column Total User's accuracy, %	6 16.7	3 33.3	17 100	13 53.8	5 20	6 83.3	28 100	12 100	90